

Does photoinhibition and/or phosphorylation of photosystem II influence its in vivo oligomeric state?

Ashraf Kitmitto ^{a,*}, Aziz O. Mustafa ^{1,a}, John W. Ford ^b, Andreas Holzenburg ^b,
Robert C. Ford ^a

^a Department of Biomolecular Sciences, UMIST, PO Box 88, Manchester M60 1QD, UK

^b Department of Biochemistry and Molecular Biology, and Department of Biology, University of Leeds, Leeds LS2 9JT, UK

Received 15 June 1999; accepted 5 July 1999

Abstract

We have examined the effects of phosphorylation and photoinhibition upon grana membranes and photosystem II (PSII) by electron microscopy and single particle analysis. No change to the overall size of PSII complexes was observed after photoinhibition. PSII centres were found to be in closer proximity to each other after phosphorylation, an effect which was reversed by photoinhibition. There were also distinct changes to thylakoid sensitivity to detergent with a reduction in (detergent-insensitive) grana membrane by up to 40% after phosphorylation and/or photoinhibition. Only minor changes to the shape and domain architecture of PSII were apparent after photoinhibition. Our data argue against the recently proposed hypothesis that photoinhibition causes a change to the oligomeric form of the complex. © 1999 Elsevier Science B.V. All rights reserved.

Keywords: Phosphorylation; Photoinhibition; Light harvesting chlorophyll *alb* protein; Single particle averaging and alignment

1. Introduction

In oxygenic photosynthesis three large protein complexes, photosystem II (PSII), the cytochrome *b₆f* complex, and photosystem I (PSI), located in the thylakoid membranes of plants and cyanobacteria, are linked in series. Together the photosystems catalyse the light-induced liberation of oxygen from water, the production of a proton gradient to drive the reduction of NADP⁺, and synthesis of ATP. PSII consists of an integral core, an oxygen-evolu-

tion enhancing complex (OEC), and light harvesting antennae. The light harvesting antennae may be subdivided into proximal and distal antennae. The proximal antennae are comprised of two chlorophyll-binding proteins (CP) CP47 (47–51 kDa) and CP43 (43–47 kDa), which are tightly coupled to the reaction core, binding chlorophyll *a* (Chl*a*) and carotene. Previous calculations based on Chl:PSII stoichiometry have suggested that about 10 light harvesting proteins per PSII complex form the distal light harvesting antenna (LHCII), around the core, covalently binding Chl*a*, Chl*b* and xanthophylls [1,2]. Electron crystallography of two dimensional (2-D) crystals of trimeric LHCII has been described at a resolution of 3.4 Å [3].

The phosphorylation/dephosphorylation cycle of

* Corresponding author. Fax: +44-161-236-0409.

¹ Present address: Department of Pharmacology, UCL, London WC1E 6BT, UK.

LHCII polypeptides provides an elegant and rapid mechanism to regulate the distribution of quanta between the two photosynthetic complexes, PSII and PSI, in response to light intensity [4–6]. The precise mechanism of protein phosphorylation for regulating the distribution of excitation energy between the two photosystems and the role in state 1–state 2 transitions [5,7–9] is unclear with a number of models proposed [10]. In a ‘molecular recognition’ theory [10] it is suggested that disruption of intramolecular and intermembrane forces by phosphorylation, leads to major structural changes by altered protein–protein interactions which provides the basis for modifying the complementarity of their respective docking surfaces. As a result of phosphorylation, phospho-LHCII dissociates from PSII, with changes to its conformation rendering binding to PSII unfavourable and so becoming free to migrate. More recently Nilsson et al. [11] have presented data which show both quaternary and tertiary structural changes to LHCII upon phosphorylation, together with the dissociation of the trimeric form. These results favour a model for the control of LHCII function based on structural changes to LHCII, upon phosphorylation, which lead to a reduction to the distance of electrostatic effects to short range, intramolecular interactions; with the tertiary structure of LHCII having a greater affinity for PSII than PSI, and the reverse for the phosphorylated form of LHCII.

There is evidence for the phosphorylation of other PSII polypeptides including the reaction centre proteins D1 and D2, CP43 and the psbH product, (a 9-kDa protein) [10]. The role of the phosphorylation of these proteins is as yet only partially understood. It has been postulated that phosphorylation of the reaction centre polypeptide D1 is to provide partial protection of PSII under high light intensities [12]. Studies have found the rate of degradation of phospho-D1 and phospho-D2 to be substantially reduced under photoinhibitory conditions [13]. However, conflicting data [14] have shown the D1 phosphoprotein preferentially degraded during photoinhibition. More recently, Kruse and co-workers [15] suggested a role for PSII protein phosphorylation as a means of stabilising PSII in a dimeric form to control the rate of D1 degradation during the photoinhibitory repair cycle. Experiments showed that solubilised PSII complexes normally isolated as dimers [16]

were isolated predominantly as PSII monomers after treatments with photoinhibitory light; whereas under phosphorylating conditions the dimeric form appeared to be stabilised.

The oligomeric nature of native PSII is still shrouded in some controversy (see [1,17] for recent reviews). A number of groups [18–23] advocate that native PSII exists as a dimer in thylakoid grana membranes. However, several other laboratories [24–28] have presented data to indicate that PSII is a monomer *in vivo*. Clearly there are inconsistencies between the different studies of PSII architecture which are discussed in some length in the cited reviews [1,17]. In the study presented here, we examine the effects of phosphorylation and photoinhibition upon both thylakoid morphology and native PSII architecture determined by electron microscopy and digital image processing. In this paper, we present evidence to challenge the hypothesis proposed by Kruse and co-workers [15] that photoinhibition influences the oligomeric state of grana PSII. We have followed the experimental procedures exactly as described previously [15] with the difference being that we have examined the photoinhibited/and or phosphorylated PSII complexes in the grana membranes as opposed to the study of Kruse et al. [15] in which photoinhibited/and or phosphorylated PSII complexes were solubilised from grana membranes (and then subsequently analysed the ratio of monomeric and dimeric complexes under each set of conditions). We have used negative staining to obtain high contrast images of the PSII grana-embedded complexes. In particular, negative stain allows visualisation of mainly those parts of the complexes extending out into the aqueous medium, thus the projection maps of grana PSII that we present are dominated by the core complex proteins; CP47, CP43, D1, D2, and extrinsic polypeptides, OEE-33 OEE-23 and OEE-16. Since LHCII polypeptides are predicted to protrude less than 1 nm out of the membrane bilayer [3], it would be expected that they would be very weakly contrasted in our images and as such not contribute much to the calculated averaged structures of PSII.

2. Materials and methods

A stock of thylakoid membranes was prepared

from commercial spinach (*Spinacia oleracea*) leaves as described previously [29]. Prior to preparation of thylakoid membranes, spinach leaves were left in the dark for 24 h at 4°C thereby promoting maximum dephosphorylation. One half of the thylakoids (batch A) was set aside in the dark at 4°C whilst the other half of the thylakoids (batch B) was phosphorylated employing conditions described by Kruse and co-workers [15] (a modified procedure of Pramanik et al. [30]).

Briefly, thylakoid membranes (batch B) were phosphorylated by suspending the membranes (at a chlorophyll concentration of 100 µg/ml) in re-suspension buffer (RSB, 20 mM MES/NaOH pH 6.0, 5 mM MgCl₂, 15 mM NaCl) containing 0.5 mM ATP, 20 mM NaF, and sodium ascorbate (0.5 g/l). Thylakoids were then incubated for 5 min in the dark followed by illumination (300 µE m⁻² s⁻¹) for 30 min at room temperature. Phosphorylation was stopped by centrifugation (10 min at 20 000 rpm, Beckman J2-21 centrifuge, JA20 rotor, at 4°C). The pellet was re-suspended with the medium above but without ATP and only 10 mM NaF. Phosphorylation of PSII phosphoproteins was confirmed by radioactive ³²P-labelling with [γ -³²P]ATP (specific activity > 148 TBq; purchased from ICN). Following this method [30] an estimated 80% of the maximum phosphorylation will have been achieved. Phosphorylated thylakoids were examined by sodium dodecyl sulphate (SDS-PAGE) polyacrylamide gel electrophoresis (4–20% gels, Bio-Rad) [31] and autoradiography of gels was performed with a Fujix BAS 1000 Phosphor-imager and quantified using the TINA V2.06b software. Several distinct bands on the autoradiogram (not shown) corresponding very closely to those shown by Kruse et al. [15] were identified with the strongest broad band between 26 and 29 kDa due to phosphorylated LHCII polypeptides.

Batch B, i.e. non-phosphorylated thylakoid membranes, were stored in absolute darkness for 30 min in the same buffer as that used for phosphorylation but without ATP or NaF.

Both batches, A and B were then divided into half, one portion put aside from each, and the other exposed to high light irradiance of 2000 µE m⁻² s⁻¹ as described in [15]. From each of the four thylakoid samples (see schematic Fig. 1) PSII enriched grana membranes, (BBYs) [32] were prepared as previously

described [29]. All buffers in contact with phosphorylated samples included 10 mM NaF. These procedures produced four BBY samples which we accordingly termed non-phosphorylated control (NPC), phosphorylated control (PC), non-phosphorylated photoinhibited (NPPI) and phosphorylated photoinhibited (PPI), as shown in Fig. 1.

Thylakoid and BBY preparations were either immediately used or stored (–80°C) in re-suspension buffer, RSB, (20 mM morpholinoethane sulphonate (MES)/NaOH pH 6.3, 5 mM MgCl₂, 15 mM NaCl) containing 20% (v/v) glycerol, or RSB containing 10 mM NaF for phosphorylated samples. Chlorophyll concentrations were determined as described by [33]. For each sample photosynthetic oxygen evolution activity was determined (see Section 3).

Average membrane area for each sample was estimated by selecting membranes from several different micrographs ($n=5$) from each data set. All membranes selected were chosen on the basis that: (a) there were no overlapping/superimposed areas; and (b) they were clearly identifiable as a separate membrane patch with the boundaries of the membrane well defined. Depending upon the shape of the membrane it was treated as a circle, square or rectangle; diameters were measured and the area calculated. For particle density measurements a boxed off area was superimposed upon each selected membrane patch and the particles falling within each area manually counted. The same boxed off area was used for all density calculations.

Aliquots of each of the BBY samples diluted to a concentration suitable for electron microscopy (EM) (20–30 (µg Chl ml⁻¹)) were mounted onto collodion-carbon-coated 300 mesh/inch copper grids and negatively stained using 4% uranyl acetate as described by Holzenburg et al. [28]. Grids were examined in a Philips CM10 transmission electron microscope operated at an accelerating voltage of 100 keV. Electron micrographs were recorded on Agfa Scientia 23D 56 electron image sheet film at calibrated magnifications of 28 500 \times g. Micrographs were digitised resulting in a pixel size of 5.1 Å at the specimen level. For single particle analysis of non-ordered PSII, SPI-DER and WEB image processing packages [34] were employed. A box size of 40 \times 40 pixels was used and from each sample 999 particles were selected (830 particles selected for PC). Using the reference-free

alignment algorithm, particles in each data set were rotationally and translationally aligned. Correspondence analysis and hierarchical ascendant classification using complete linkage as a merging criterion were performed to separate out and average particles in each sample group. The threshold level was determined by visual inspection of particles randomly selected from each group to check for agreement of particle orientation, shape and size.

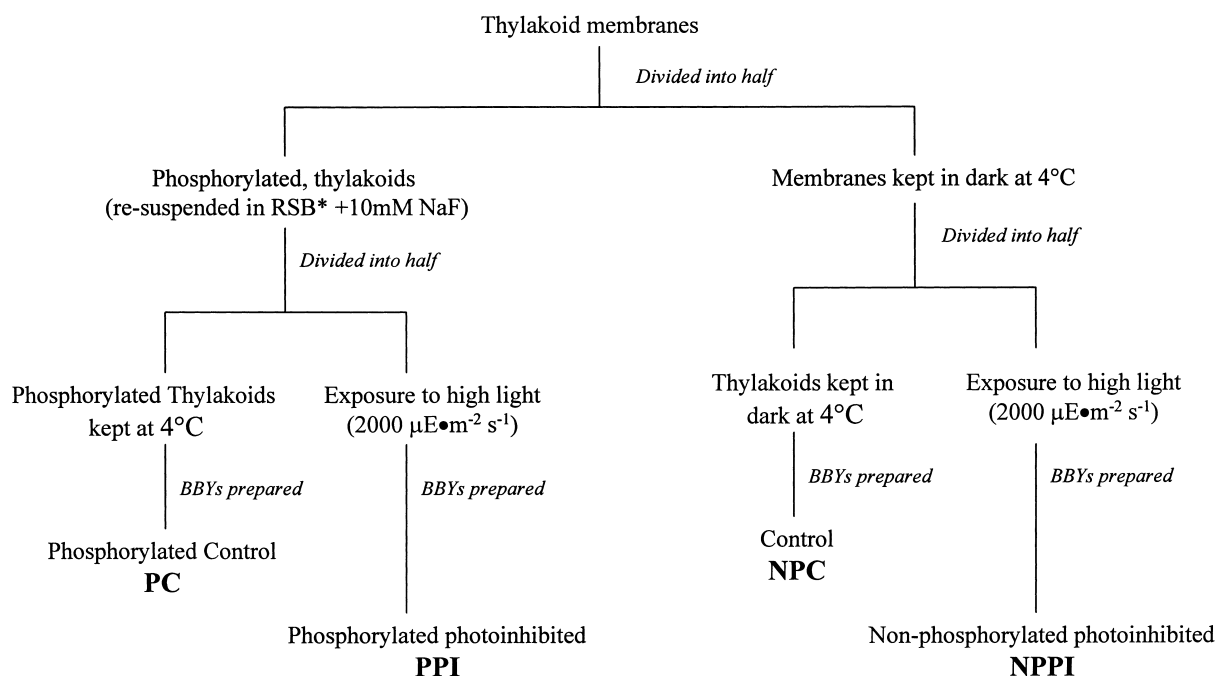
Resolution assessment of the final averaged images (for each sample type) was determined by plotting differential phase residual (DPR) and Fourier ring correlation (FRC) between two independent averages against spatial frequency. A cut-off of 45° was taken as a conservative measure of resolution for DPR and $1/\sqrt{N}$ for FRC where N is the number of comparisons within the given Fourier ring [35].

3. Results

Electron micrographs of negatively stained grana

membranes from each of the samples; non-phosphorylated control (NPC), phosphorylated control (PC), non-phosphorylated photoinhibited (NPPI) and phosphorylated photoinhibited (PPI), are shown in Fig. 2A–D, respectively. Control (NPC) membranes (Fig. 2A) are typical of BBYs previously isolated in this laboratory with large continuous membrane sheets containing stain-excluding PSII protein complexes [36]. In contrast, the grana membranes of PC, NPPI and PPI (Fig. 2B–D, respectively) were found to be smaller as shown in Fig. 3. Detailed measurements showed a 25–60% reduction to the area of isolated grana membranes after phosphorylation or after photoinhibition of control thylakoids (Fig. 3). However, when phosphorylated membranes were subsequently exposed to high light irradiance no further reduction in grana membrane area was found.

The density of PSII in the grana membranes (number of stain-excluding particles per μm^2 of membrane) was determined after each treatment, as presented in Fig. 3. After phosphorylation there was a



* RSB = 20mM MES/NaOH pH 6.3, 5mM MgCl₂, 15mM NaCl

Fig. 1. Schematic representation of sample preparation employed in this work. Detailed methods are given in the main text (see Section 2).

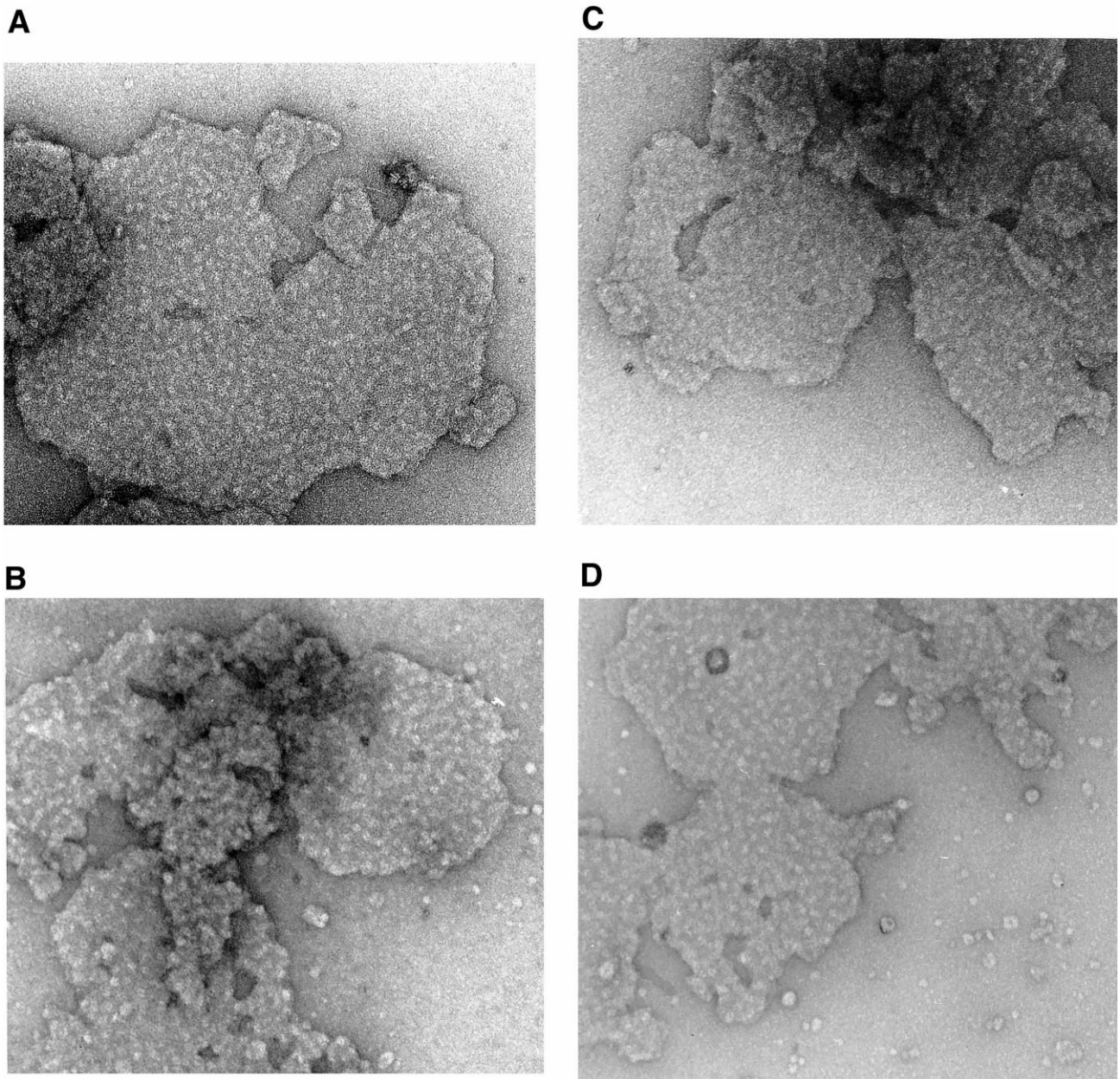


Fig. 2. Electron micrographs of negatively stained grana: (A) control (NPC); (B) photoinhibited (NPPI); (C) phosphorylated (PC); (D) phosphorylated and photoinhibited (PPI). Scale bar: 200 nm.

significant increase ($P < 0.002\%$) in particle density (ranging between +20 and +42%) as compared to control (NPC) samples. We found that photoinhibition of non-phosphorylated thylakoids did not significantly affect grana PSII density ($P > 0.1\%$), but in contrast photoinhibition of phosphorylated thylakoid membranes resulted in a reduction in PSII den-

sity in grana membranes by between 31 and 43% ($P < 0.001\%$).

Oxygen evolution activities of each sample were measured. Phosphorylation of thylakoids led to a 23% reduction in oxygen evolution compared to control (NPC) membranes. After exposure of both control and phosphorylated thylakoid membranes to

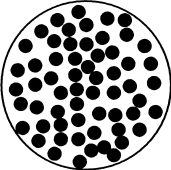
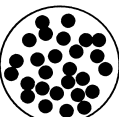
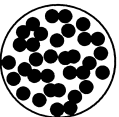
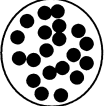
Schematic representation of membrane area and PSII density data (Circles represent membrane areas; black dots PSII complexes)				
Sample treatment	NPC	NPPI	PC	PPI
Average size of grana membranes (μm^2) (n=5)	0.39 \pm 0.08	0.19 \pm 0.04	0.17 \pm 0.01	0.16 \pm 0.01
PSII density: No. of particles / μm^2 (n=5)	3089 \pm 203	2802 \pm 82	4043 \pm 135	2548 \pm 127

Fig. 3. Average grana membrane size (μm^2) and mean PSII density (μm^{-2}) for the four different preparations represented graphically and numerically. NPC, non-phosphorylated control; NPPI, non-phosphorylated photoinhibited; PC, phosphorylated control; PPI, phosphorylated photoinhibited.

high light irradiance for 30 min there was a loss of virtually all oxygen evolving capacity in the grana suggesting that PSII was fully photoinhibited.

Presented in Fig. 4a–d are projection maps generated by single particle alignment and averaging of particles selected from micrographs of each sample. Hierarchical classification showed that in each data-set there was a relatively homogeneous population of PSII complexes, and in each case the average was generated from over 90% of the total particles selected (see Table 1). A homogeneity in terms of complex orientation and staining would be expected since the PSII complexes are embedded within the grana lipid bilayer and as such movement of the complexes would be restricted in the direction perpendicular to the membrane. The control (NPC) map shows a distinct resemblance to previous maps of PSII (a clearly defined central cavity surrounded by four or five protein domains) as determined from 2-D crystals [25,37] and by single particle analysis of non-ordered PSII [26,38]. Domains I–V are labelled on the projection maps in Fig. 4 according to the assignment by Holzenburg et al. [25,36,39]. After exposure to phosphorylating conditions, minor changes to the overall shape of the averaged PSII complex were observed. The central cavity in the projection map of phosphorylated samples (Fig. 4b) is still well defined though there are some apparent changes to the protein domains surrounding the cavity. These changes

result in a more pronounced ‘wedge’ shape to the lower half of the complex in the figure and a reduction in the pseudosymmetrical appearance of the complex. Similar changes have previously been observed after partial removal of the oxygen evolution-enhancing subunits, OEE II (23 kDa) and OEE III (16 kDa), by mild salt treatment [39]. Similarly, the projection maps for the photoinhibited (NPPI) and phosphorylated photoinhibited (PPI) PSII show a more pronounced wedge shape and are suggestive of the partial loss or rearrangement of domains II and III. However, in all maps, domains I, IV and V appear to be present. In both phosphorylated (PC) and phosphorylated photoinhibited (PPI) PSII (Fig. 4b,d) there appears to be a small migration of domain I to a position close to the mid-line of the complex.

Since there remains much contention as to whether PSII exists as a monomer or dimer we have also presented the averaged projection maps of the PSII complexes (Fig. 4a–d) after applying a two-fold symmetry operation, see Fig. 5a–d. As would be expected there is no real change to the overall size of the averaged PSII complexes (control and treated) as compared to the non-symmetrised projection maps. By taking the closely spaced contours as delineating the boundaries of the complexes, the dimensions of PSII after each treatment (Fig. 4a–d) were calculated (Table 1). There were no significant changes to the

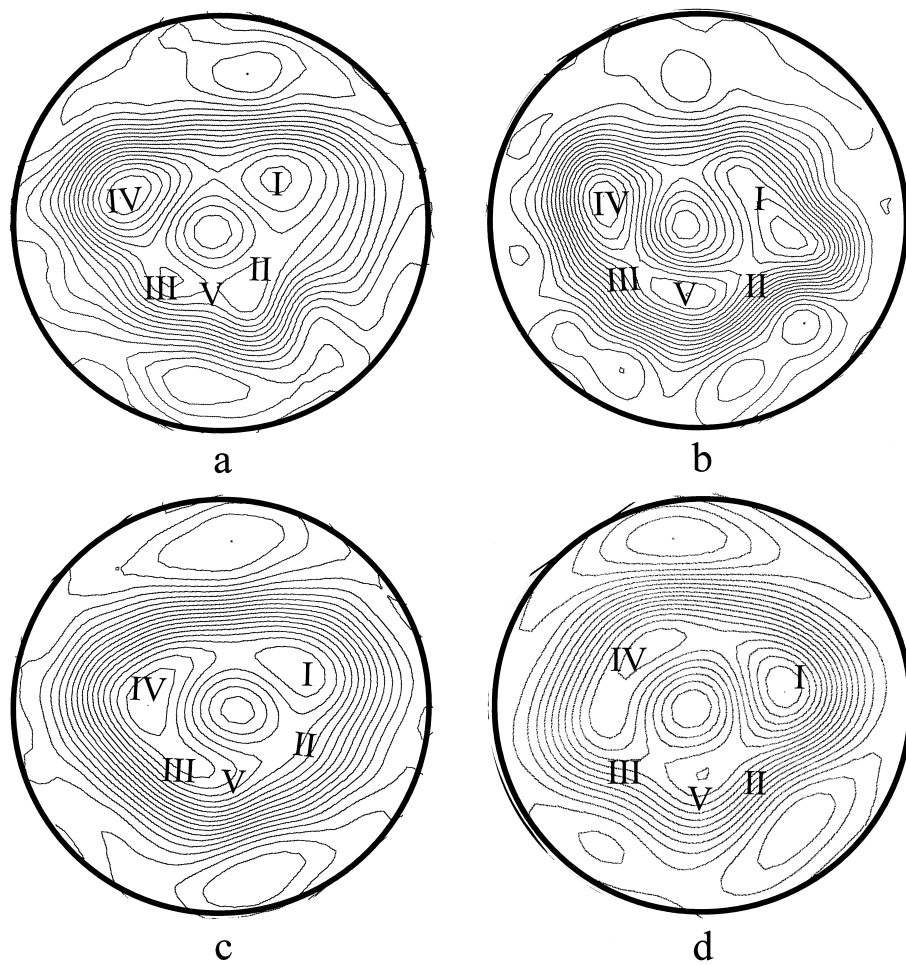


Fig. 4. Average projection maps of grana PSII complexes from each of the samples: (a) control (NPC); (b) phosphorylated (PC); (c) photoinhibited (NPPI); and (d) phosphorylated and photoinhibited (PPI). Scale bar: 5 nm.

Table 1
Particle dimensions and resolution estimates of averaged projection maps

Sample treatment	Particle dimensions (nm) ^a	Class size (% of total particles selected)	Estimated resolution limit (nm)	
			DPR ^b	FRC ^c
NPC	12.9 × 17.5	90	3.4	2.6
NPPI	13.4 × 18.3	94	3.7	2.5
PC	13.4 × 17.8	92	3.1	2.4
PPI	12.7 × 18.3	94	3.5	2.3

NPC, non-phosphorylated control; NPPI, non-phosphorylated photoinhibited; PC, phosphorylated control; PPI, phosphorylated photoinhibited.

^aAs determined from the projection maps in Fig. 3.

^bDPR, differential phase residual.

^cFRC, Fourier ring correlation.

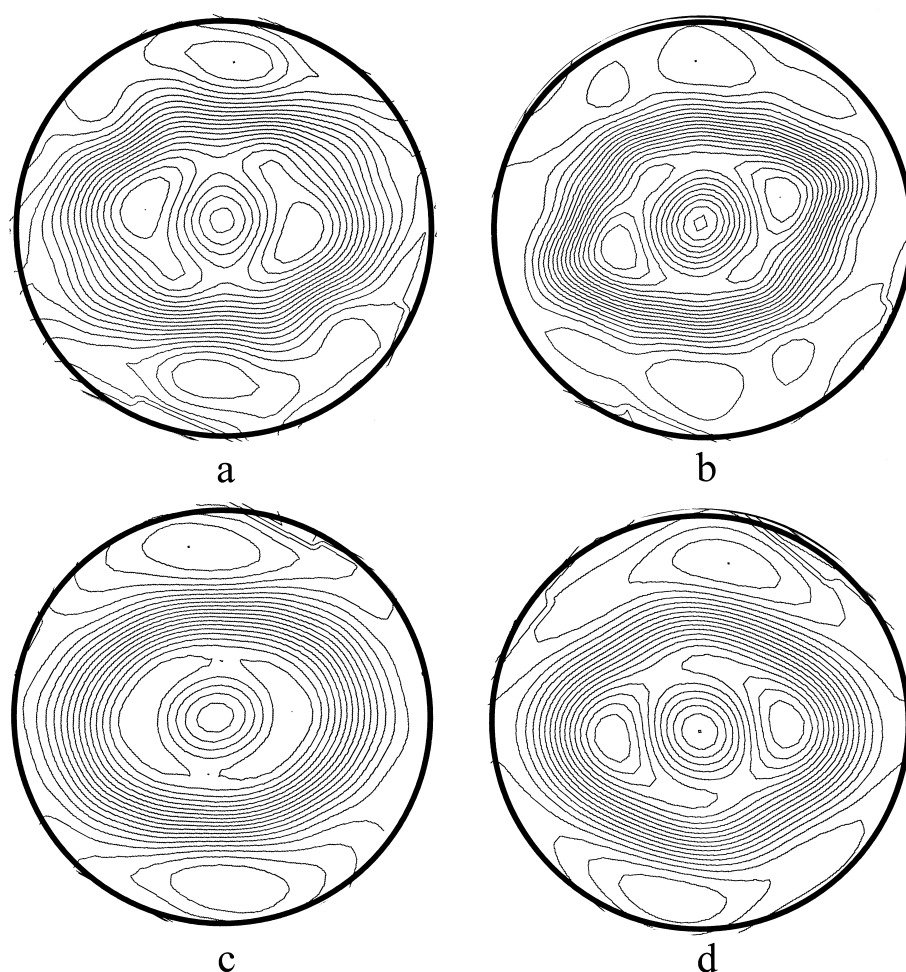


Fig. 5. Average projection maps of PSII complexes from each sample type after two-fold rotational symmetry has been imposed: (a) control (NPC); (b) phosphorylated (PC); (c) photoinhibited (NPPI); and (d) phosphorylated and photoinhibited (PPI). Scale bar: 5 nm.

overall dimensions of any of the averaged molecules with dimensions of, 13.4×18.3 nm (NPPI), 13.4×17.8 nm (PC), 12.7×18.3 nm (PPI), when compared to the control (NPC) 12.9×17.5 nm.

4. Discussion

The role of protein migration in the thylakoid membrane has been correlated to several events, such as state transitions, protein turnover and repair of PSII [10]. Changes to thylakoid domain organisa-

tion as a function of phosphorylation state have been documented [40–43]. However, the reduction to grana membrane area reported here of between 25 and 60%, after phosphorylation, is greater than that determined previously. For example, Kyle et al. [42] showed only a 23% reduction to the area of stacked membranes after phosphorylation as determined by freeze fracture. In addition, the reduction in area reported here is much larger than the area expected to be occupied by the phospho-LHCII complexes [40]. These large changes would seem to support the phosphorylation model proposed by Barber [44]

involving the intermixing of PSII with PSI as a result of grana unstacking. However, the extent of solubilisation of membranes by detergent treatment after phosphorylation of LHCII is likely to be dependent on several factors including the extent of destacking of the grana. Thus effects of phosphorylation and photoinhibition studied here may well have resulted in greater sensitivity of the thylakoid membranes to detergent.

Particle density measurements show a closer packing of the phosphorylated PSII complexes. This is consistent with the idea of migration of phospho-LHCP complexes away from the grana membranes. This would result in a population of PSII complexes with a depleted distal antenna and thus motion in the plane of the membrane would allow PSII complexes to come closer together. Since LHCII polypeptides are believed to be in part responsible for the stabilisation of grana stack structure then this migration might also result in an unravelling of the stacks leading to greater sensitivity to detergent (as discussed earlier). Photoinhibition of control thylakoids showed no significant changes to the density of PSII complexes, but rather a change in membrane area.

The projection maps of the averaged PSII complexes in the grana membranes (Fig. 4) showed no large changes to the overall dimensions of the PSII complexes after phosphorylation or photoinhibition. According to the hypothesis put forward by Kruse and co-workers [15], we would predict a reduction to one of the dimensions of the NPPI averaged PSII complex (Fig. 4c) by one half when compared to the control (Fig. 4a). Clearly this is not the case. Furthermore, close examination of the 6% of particles excluded from merging found no sub-group with dimensions which could be likened to a PSII population with dimensions half the size of control (NPC) PSII complexes (Fig. 4a). The approximate dimensions of control PSII 13×17.5 nm are very close to those previously reported for core PSII complexes [37]. These dimensions are, however, smaller in comparison to previous reports for the unit cell dimensions of native PSII, from this laboratory, of 17×19 nm determined from studies of native 2-D crystals. As discussed earlier (see Section 1) we would not expect the LHCII polypeptides to be readily visualised and thus contribute to the calculated averaged structure. Therefore, it would be reasonable to

predict that the projection maps presented here more closely represent averaged core PSII complexes, i.e. LHCII depleted. Though the same argument holds true for studies of native negatively stained PSII 2-D arrays it is believed that the LHCII polypeptides are involved in forming the lattice structure in the 2-D crystals (see [1]) which leads to a calculation of a larger unit cell.

Although it has been suggested that photodamaged PSII complexes migrate to the non-appressed regions [45] of the thylakoid and that those in the grana may represent an undamaged PSII population, albeit inactive, it should be emphasised that the purpose of this investigation was to test a hypothesis [15], in which the subject of study was grana PSII. Analyses of stromal membranes for photodamaged PSII complexes would therefore be an interesting avenue to pursue for a logical continuation of this work. A key consideration when considering this data in context with that presented earlier [15] is that here we have studied the effects of phosphorylation and photoinhibition upon native PSII complexes. We suggest that in the study of Kruse and co-workers conformational changes to solubilised PSII complexes under phosphorylating conditions work to stabilise the detergent-induced dimer (normally isolated under their described experimental conditions [16]) when exposed to high light intensities.

Acknowledgements

The authors would like to thank Mr P. McPhie and Mr J. Mallet for technical support. We also wish to thank the BBSRC, the Academic Development Fund of the University of Leeds and The Leeds Centre for Molecular Recognition in Biological Sciences, for financial support of this work.

References

- [1] W.V. Nicholson, R.C. Ford, A. Holzenburg, *Biosci. Rep.* 16 (1996) 159–187.
- [2] S. Jansson, *Biochem. Biophys. Acta* 1184 (1994) 1–19.
- [3] W. Kühlbrandt, D.N. Wang, Y. Fujiyoshi, *Nature* 367 (1994) 614–621.

- [4] J. Barber, *Photobiochem. Photobiophys.* 5 (1983) 181–190.
- [5] J. Bennett, K.E. Steinback, C.J. Arntzen, *Proc. Natl. Acad. Sci. USA* 77 (1980) 5253–5257.
- [6] P. Horton, M.T. Black, *FEBS Lett.* 119 (1980) 141–144.
- [7] P. Horton, M.T. Black, *Biochim. Biophys. Acta* 635 (1981) 53–62.
- [8] G. Forti, P. Fusi, *Biochim. Biophys. Acta* 1020 (1980) 247–252.
- [9] W.L. Butler, *Annu. Rev. Plant Physiol.* 29 (1978) 345–378.
- [10] J.F. Allen, *Biochim. Biophys. Acta* 1098 (1992) 275–335.
- [11] A. Nilsson, S. Dalibor, T. Drakenberg, M.D. Spangfort, S. Forsén, J.F. Allen, *J. Biol. Chem.* 272 (1997) 18350–18357.
- [12] E.M. Aro, S. McCaffery, J.M. Anderson, *Plant Physiol.* 103 (1993) 835–843.
- [13] E. Rintamäki, R. Kettunen, E. Tyystäarvi, E.-M. Aro, *Physiol. Plant.* 93 (1995) 191–195.
- [14] T.D. Elich, M. Edelman, A.K. Mattoo, *J. Biol. Chem.* 267 (1992) 3523–3529.
- [15] O. Kruse, D. Zheleva, J. Barber, *FEBS Lett.* 408 (1997) 276–280.
- [16] B. Hankamer, J. Barber, E.J. Boekema, *Annu. Rev. Plant Physiol. Plant Mol. Biol.* 48 (1997) 641–671.
- [17] M. Rögner, E.J. Boekema, J. Barber, *Trends Biochem. Sci.* 21 (1996) 44–49.
- [18] K.H. Rhee, E.P. Morris, J. Barber, W. Kuhlbrandt, *Nature* 396 (1998) 283–286.
- [19] K.H. Rhee, E.P. Morris, D. Zheleva, B. Hankamer, W. Kuhlbrandt, J. Barber, *Nature* 389 (1997) 522–526.
- [20] M.K. Lyon, *Biochem. Biophys. Acta* 1364 (1998) 403–419.
- [21] K.M. Marr, D.N. Mastrorade, M.K. Lyon, *J. Cell Biol.* 132 (1996) 823–833.
- [22] K. Nakazato, C. Toyoshima, I. Enami, Y. Inoue, *J. Mol. Biol.* 257 (1996) 225–232.
- [23] E.J. Boekema, B. Hankamer, D. Bald, J. Kruip, J. Nield, A.F. Boonstra, J. Barber, M. Rögner, *Proc. Natl. Acad. Sci. USA* 92 (1995) 175–179.
- [24] S.S. Stoylova, T.D. Flint, R.C. Ford, A. Holzenburg, *Micron* 28 (1997) 439–446.
- [25] S.S. Stoylova, T.D. Flint, A. Kitmitto, R.C. Ford, A. Holzenburg, *Micron* 29 (1998) 341–348.
- [26] L. Hasler, D. Ghanotakis, B. Fedtke, A. Spyridaki, M. Miller, S.A. Muller, A. Engel, G. Tsiotis, *J. Struct. Biol.* 119 (1997) 273–283.
- [27] G. Tsiotis, T. Walz, A. Spyridaki, A. Lustig, A. Engel, D. Ghanotakis, *J. Mol. Biol.* 259 (1996) 241–248.
- [28] A. Holzenburg, F.H. Shepherd, R.C. Ford, *Micron* 25 (1994) 447–451.
- [29] R.C. Ford, M.C.W. Evans, *FEBS Lett.* 160 (1983) 159–164.
- [30] A.M. Pramanik, S. Bingsmark, M. Lindahl, H. Baltscheffsky, M. Baltscheffsky, B. Andersson, *Eur. J. Biochem.* 198 (1991) 183–186.
- [31] U.K. Laemmli, *Nature* 227 (1970) 680–685.
- [32] D.A. Berthold, G.T. Babcock, C.F. Yocum, *FEBS Lett.* 153 (1981) 231–234.
- [33] D.I. Arnon, *Plant Physiol.* 24 (1949) 1–15.
- [34] J. Frank, M. Radermacher, P. Penczek, J. Zhu, Y.H. Li, M. Ladjadj, A. Leith, *J. Struct. Biol.* 116 (1996) 190–199.
- [35] M. van Heel, *Ultramicroscopy* 21 (1987) 95–100.
- [36] W.V. Nicholson, F.H. Shepherd, M.F. Rosenberg, R.C. Ford, A. Holzenburg, *Biochem. J.* 315 (1996) 543–547.
- [37] A. Holzenburg, M.C. Bewley, R.H. Wilson, W.V. Nicholson, R.C. Ford, *Nature* 363 (1993) 470–472.
- [38] M.F. Rosenberg, A. Holzenburg, F.H. Shepherd, W.V. Nicholson, T.D. Flint, R.C. Ford, *Biochim. Biophys. Acta* 1319 (1997) 119–132.
- [39] A. Holzenburg, T.D. Flint, F.H. Shepherd, R.C. Ford, *Micron* 27 (1996) 121–127.
- [40] H. Stefansson, L. Wollenberger, S.G. Yu, P.-A. Albertsson, *Biochim. Biophys. Acta* 1231 (1995) 323–334.
- [41] A. Telfer, M. Hodges, P.A. Millner, J. Barber, *Biochim. Biophys. Acta* 766 (1984) 554–562.
- [42] D.J. Kyle, L.A. Staehelin, C.J. Arntzen, *Arch. Biochem. Biophys.* 222 (1983) 527–541.
- [43] U.K. Larsson, B. Jergil, B. Andersson, *Eur. J. Biochem.* 136 (1983) 25–29.
- [44] J. Barber, *Annu. Rev. Plant Physiol.* 33 (1982) 261–295.
- [45] E.-M. Aro, I. Virgin, B. Andersson, *Biochim. Biophys. Acta* 1143 (1993) 113–134.